Graphene Functionalization | Hot Paper

International Edition: DOI: 10.1002/anie.202002508
German Edition: DOI: 10.1002/ange.202002508

Spatially Resolved Bottom-Side Fluorination of Graphene by Two-Dimensional Substrate Patterning

*Lipiao Bao, Baolin Zhao, Vicent Lloret, Marcus Halik, Frank Hauke, and Andreas Hirsch**

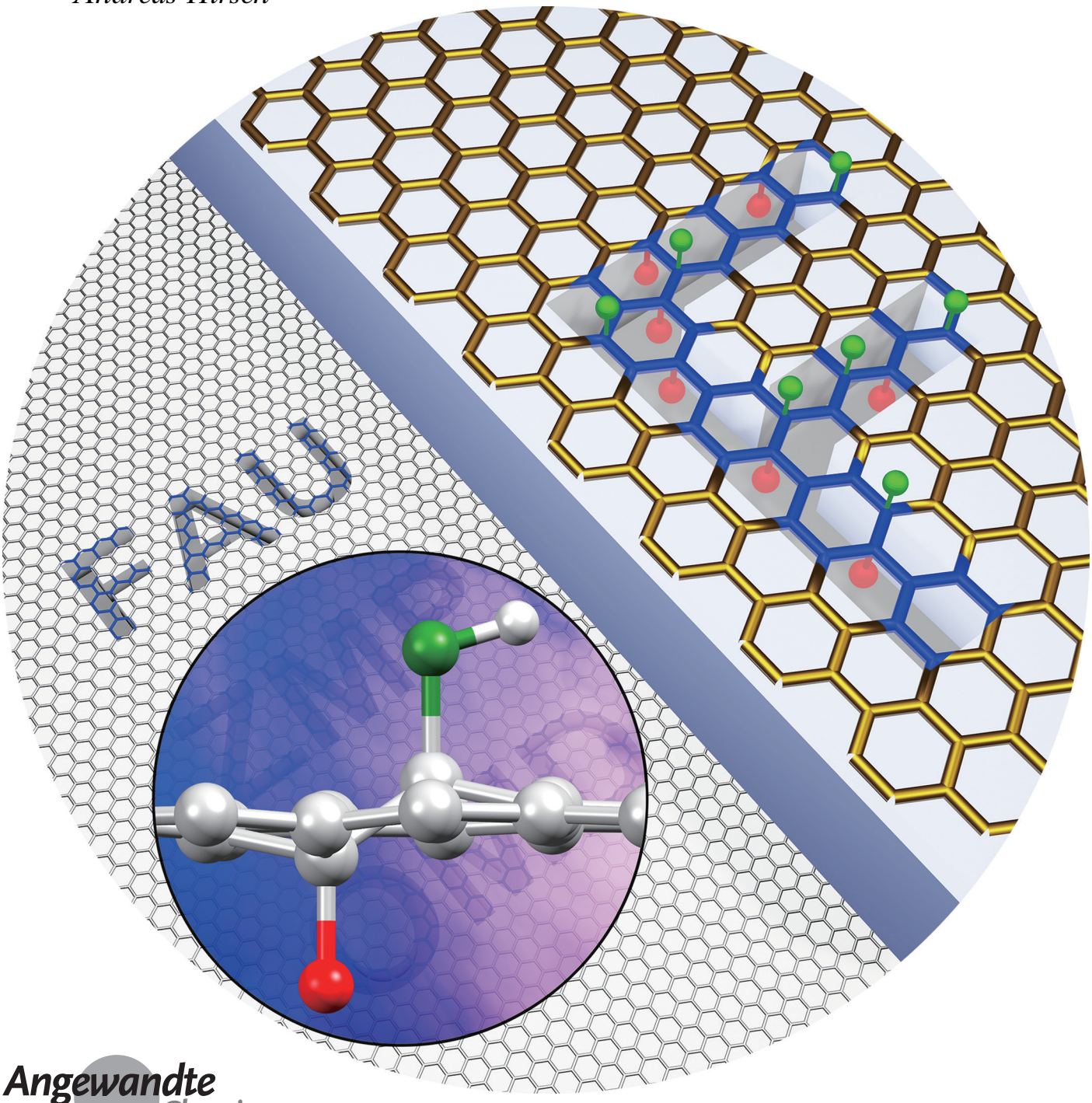

 © 2020 The Authors. Published by Wiley-VCH Verlag GmbH & Co. KGaA, Weinheim

Abstract: *Patterned functionalization can, on the one hand, open the band gap of graphene and, on the other hand, program demanding designs on graphene. The functionalization technique is essential for graphene-based nanoarchitectures. A new and highly efficient method was applied to obtain patterned functionalization on graphene by mild fluorination with spatially arranged AgF arrays on the structured substrate. Scanning Raman spectroscopy (SRS) and scanning electron microscopy coupled with energy-dispersive X-ray spectroscopy (SEM-EDS) were used to characterize the functionalized materials. For the first time, chemical patterning on the bottom side of graphene was realized. The chemical nature of the patterned functionalization was determined to be the ditopic scenario with fluorine atoms occupying the bottom side and moieties, such as oxygen-containing groups or hydrogen atoms, binding on the top side, which provides information about the mechanism of the fluorination process. Our strategy can be conceptually extended to pattern other functionalities by using other reactants. Bottom-side patterned functionalization enables utilization of the top side of a material, thereby opening up the possibilities for applications in graphene-based devices.*

Well-defined graphene nanoarchitectures engineered by patterning the confined surface areas of graphene have a highly attractive potential in various fields of applications, such as molecular electronics and catalysis.[1–4] However, such structures requires facile and flexible synthetic methods for the rational design of spatially resolved two-dimensional (2D) patterning of graphene. In preceding reports, graphene patterning has been accomplished by two general approaches: 1) etching away selected parts of the graphene lattice in a top-down manner[5–7] or bottom-up surface assisted polymerizations of aromatic precursors to form nanoribbons,[8] and 2) covalent surface patterning of addends on defined areas of the graphene basal plane.[9–14] The latter method allows for combining the outstanding properties of graphene with those of other compound classes. The latter approach can, in general, be realized by combining graphene chemistry with established patterning techniques, such as lithography and laser/plasma writing. Typically, predefined poly(methyl methacrylate) (PMMA) masks prepared by lithography are used to direct covalent functionalization to occur only in the unprotected regions of exposed graphene. In this way, hydrogenations, reactions with diazonium salts,[9] and additions of *cis*-dienes[10] have been performed to generate addend structured graphene. However, so far the corresponding addend patterned areas are characterized by a relatively low degree of functionalization; for example, the Raman features are located in the low-functionalization regime of the Cançado curve.[15] This drawback was also observed for the reported force-accelerated stamping method.[11] Alternatively, laser/plasma-write techniques were applied to obtain a high degree of patterned functionalization on graphene.[12,13] These methods require a laser-trigged reaction with related laser equipment or a suitable plasma source, which limits the scope of the sequences. Thus, new, efficient and easy-to-perform methods are still highly desired for the patterned 2D functionalization of graphene.

Herein we report a new and highly efficient method for the covalent 2D patterning of graphene. For the first time, we carried out a bottom-side fluorination of graphene by using 2D patterned substrates containing spatially arranged AgF arrays serving as a mild fluorination source. A very high degree of covalent functionalization was obtained by allowing for antaratopic top-side reactions; for example, from adsorbed water layers quenching the initially formed dangling bonds in *trans* positions (Scheme 1 d). This leads to strain-free

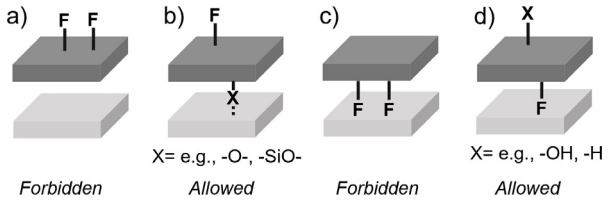

Scheme 1. Possible binding topologies of graphene derivatives supported on a solid substrate. a) Supratopic top-side addition, b) top-side initiation with antaratopic quenching by interlayer molecules, such as water or non-inert substrates, c) supratopic bottom-side addition, and d) bottom-side addition with antaratopic quenching by molecules located at the top side (for example, water coverages).

sp^3 regions within the hexagonal C-lattice. This strategy could be easily extended to pattern other functionalities on graphene by using other reactants. To date, all the reported patterned graphene derivatizations have been based on top-side chemistry opposite to the underlying substrate.[9–13] Notably, exclusive supratopic addition sequences (Schemes 1 a,c) on graphene are not allowed because an enormous amount of strain energy would be built up (eclipsing addend interactions, the planar cyclohexane ring, dramatic sheet bending, and loss of contact with the substrate).[16,17] Antaratopic quenching (X addend from the opposite side of the basal plane of graphene, Schemes 1 b,d) requires the availability of either reactive substrates or adjacent molecules, such as a water layer. Binding of addends from both sides is hindered by direct contact of graphene with the substrate but

[*] Dr. L. Bao, V. Lloret, Dr. F. Hauke, Prof. Dr. A. Hirsch
Department of Chemistry and Pharmacy & Joint Institute of Advanced Materials and Processes (ZMP)
Friedrich-Alexander University of Erlangen-Nürnberg
Nikolaus-Fiebiger-Strasse 10, 91058, Erlangen (Germany)
E-mail: andreas.hirsch@fau.de
B. Zhao, Prof. Dr. M. Halik
Organic Materials and Devices (OMD), Institute of Polymer Material Interdisziplinären Zentrums für Nanostrukturierte Filme (IZNF)
Friedrich-Alexander University of Erlangen-Nürnberg
Cauerstraße 3, 91058 Erlangen (Germany)
Supporting information and the ORCID identification number(s) for the author(s) of this article can be found under: https://doi.org/10.1002/anie.202002508.

© 2020 The Authors. Published by Wiley-VCH Verlag GmbH & Co. KGaA. This is an open access article under the terms of the Creative Commons Attribution Non-Commercial NoDerivs License, which permits use and distribution in any medium, provided the original work is properly cited, the use is non-commercial, and no modifications or adaptations are made.

is possible if 1) the addend can travel around edges or through extended hole defects in the basal plane, or 2) the reaction is carried out in solution.[1,18,19] Our approach includes the possibility of Janus-type patterned functionalization, which has not been realized to date, although unpatterned Janus graphene has been accomplished in a step-by-step procedure[20] or simultaneously by trapping the starting graphene at the liquid–liquid interface.[21] Remarkably, the mild fluorination approach shown here is reasonably facile, whereas the methods reported to date generally involve hazardous gases (F_2 or XeF_2),[22,23] or expensive plasma or laser equipment.[12,24]

Our patterning process, initiated by bottom-side additions from the structured substrate, is described in Scheme 2. Briefly, predefined channels were first introduced onto a Si/SiO_2 wafer using lithography. AgF was then specifically trapped in these channels. Subsequently, monolayer graphene covered by PMMA was transferred onto the prepared wafer. The F-patterning on the bottom side was initiated by heating at 100 °C for 30 seconds. The PMMA layer was then removed using acetone.

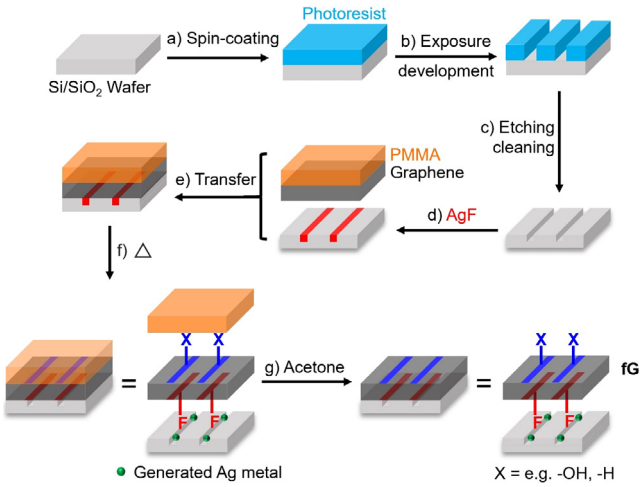

Scheme 2. Illustration of the 2D substrate patterning leading to structured bottom-side fluorination on graphene. a) The positive photoresist layer (S1813) was spin-coated on a Si/SiO_2 wafer. b) The desired pattern was realized on the photoresist film by exposure through a Cr mask under 365 nm UV light and developed in a diluted UN1824 solution (NaOH). c) The exposed silicon oxide was etched by buffered ammonium fluoride/hydrofluoric acid (v/v = 7:3), followed by cleaning with acetone to afford the predefined channels on the Si/SiO_2 wafer. d) An AgF water solution (0.05 mmol mL^{-1}) was specifically trapped in these channels using a needle and visualized under a microscope. e) Monolayer graphene was transferred onto the wafer. f) The wafer was heated at 100 °C for 30 s. g) The PMMA layer was removed using acetone.

To determine the patterned graphene functionalization we first carried out systematic Raman spectroscopy investigations. Figure 1a shows the typical Raman spectrum of pristine monolayer graphene before functionalization with a G-band at 1582 cm^{-1} (sp^2 lattice carbon atoms) and a negligible defect-induced D-band at 1350 cm^{-1}. After the thermal treatment with AgF, the Raman spectrum for the

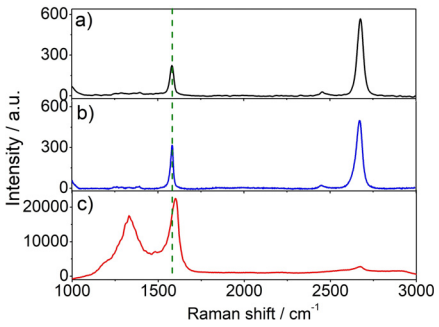

Figure 1. Raman spectra of a) starting graphene, b) unpatterned areas, and c) patterned regions after functionalization; $\lambda_{exc} = 532$ nm.

unpatterned regions remains intact with an I_D/I_G ratio of < 0.1 (Figure 1b), showing unaffected graphene regions. In contrast, for the patterned area the D-band is very broad and the 2D band almost vanished. This is a direct indication of a very high degree of functionalization and it shows that we are on the high-functionalization regime of the Cançado curve.[15] Consistently, the G-band at the patterned area is observed at 1600 cm^{-1}, corresponding to an upshift relative to that of the unpatterned regions (1582 cm^{-1}) owing to the covalent attachment of electron-withdrawing fluorine atoms in the functionalized areas.[25] Successful fluorination is further demonstrated by the reaction of exfoliated graphene with AgF (Supporting Information). The G-band intensity for patterned areas is significantly enhanced and reaches over 50 times that of unpatterned regions as a result of the enhancement of Raman scattering by the Ag metal generated in patterned areas after the reaction (Supporting Information, Figures S4, S6, and S7).[26]

As a prototype, a specific letter pattern "OMD" (Figure 2a) was generated on the wafer. After the reaction, patterned OMD-functionalized graphene (**fG**) was obtained.

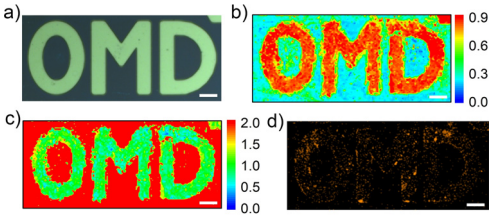

Figure 2. a) Optical image of the "OMD" pattern on the substrate, b) Raman I_D/I_G mapping, and c) Raman I_{2D}/I_G mapping of **fG**; $\lambda_{exc} = 532$ nm. d) SEM-EDS mapping of F in **fG**; scale bar = 50 μm.

To visualize the chemical pattern, Raman mapping and scanning electron microscopy coupled with energy-dispersive spectroscopy (SEM-EDS) were conducted. Raman I_D/I_G and I_{2D}/I_G maps (Figures 2b,c) clearly show that the functionalization selectively took place at the regions where predefined channels were located on the substrate. Furthermore, the functionalization at the patterned area is homogeneous. This patterned fluorination is further supported by the matching F

 © 2020 The Authors. Published by Wiley-VCH Verlag GmbH & Co. KGaA, Weinheim

and Ag distributions in the SEM-EDS images (Figure 2d; Supporting Information, Figure S6).

The thermal stability of the patterned fluorination was investigated by temperature-dependent Raman spectroscopy. As shown in Figure 3, only a minor decrease of the Raman I_D/I_G ratios was observed below 250 °C, suggesting high stability in this temperature range. Further increasing the temperature to 400 °C resulted in a sharp decline of the Raman I_D/I_G ratio accompanied by the complete disappearance of the characteristic Raman features (D-, G-, and 2D-bands). This demonstrates the complete destruction of the graphene framework upon heating to 400 °C as a consequence of the very high degree of functionalization.[22]

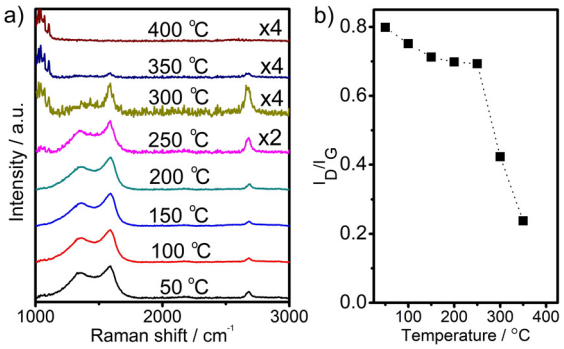

Figure 3. a) Temperature-dependent Raman spectra of the patterned area of **fG** and b) the mean Raman I_D/I_G ratio extracted from temperature-dependent Raman spectra; $\lambda_{exc} = 532$ nm. These spectra have been magnified for clarity.

With this new 2D substrate patterning method, we have initiated the graphene functionalization by spatially resolved fluorination from the bottom side of graphene. The question is: what happened on the top side during this process? In principle, three scenarios can be considered after the initial addition of fluorine radicals has taken place (Figure 4):

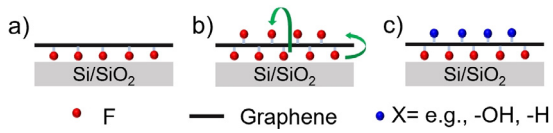

Figure 4. Possible configurations of **fG**. a) Supratopic fluorination (**Config-a**), b) antaratopic fluorination with possible transportation routes of fluorine atoms indicated by green arrows (**Config-b**), and c) fluorine atoms on the bottom side with antaratopic quenching by hydroxy groups or hydrogen atoms on the top side (**Config-c**).

1) no top-side additions at all (**Config-a**), 2) antaratopic fluorine additions provided by migrations of F from the bottom side through σ-holes in the basal plane or around the entire graphene flake (**Config-b**), and 3) quenching reactions with molecules located at the top side, such as H_2O or O_2 (**Config-c**).

As pointed out in the preceding text, the high degree of functionalization reported herein can only be realized if antaratopic reactions are involved. Hence, **Config-a** is directly ruled out because addition from one side must always be accompanied by an addition to the other side.[16,17] Our Raman studies imply that **Config-b** is unlikely because, during a normal fluorination procedure that allows for attacks on both sides of the basal graphene, reaction products are generated with Raman spectra that are almost featureless and lack the characteristic signatures of graphene. In particular, very weak or even absent D- and G-bands are noted and, instead, a very broad and unstructured low-intensity peak at 1000–3000 cm^{-1} is observed, which was attributed to the fluorescence of the highly fluorinated graphene.[25] In our case, the characteristic Raman spectrum for highly fluorinated graphene (Figure 5a) is found for very few spots

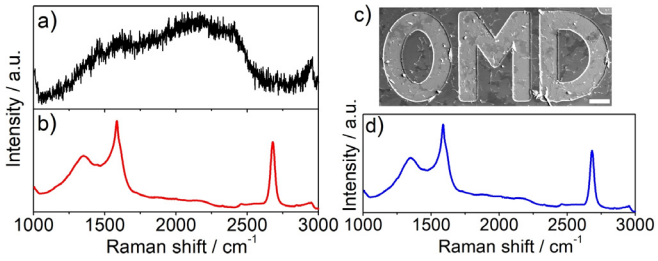

Figure 5. a) Single-point Raman spectrum of selected spots of **fG** and b) mean Raman spectrum of **fG**. c) The SEM image and d) mean Raman spectrum of **fG-Hi**; $\lambda_{exc} = 532$ nm, scale bar = 50 μm.

(approximately five out of 9570 single-point Raman spectra for the entire mapping area shown in Figure 2). Moreover, no fluorescence signal is seen, but a very pronounced D-band appears in the mean Raman spectrum of the entire mapping area (Figure 5b). Ditopic fluorination with a low degree of functionalization was excluded by a control experiment with a 120-fold longer reaction time (1 h) and a 10-fold higher amount of AgF compared to **fG**, affording **fG-Hi**. As seen in the SEM image (Figure 5c), many cracks or holes were generated during the formation of **fG-Hi**. The defects could provide channels for transferring fluorine (for example, from the bottom side to the top side), leading to a high degree of fluorination on both sides. However, the mean Raman spectrum of **fG-Hi** (Figure 5d) resembles that of **fG** (Figure 5b), suggesting that the reaction sites of carbon atoms on both sides in **fG** are already saturated.

Config-b is further excluded by testing a potential substitution reaction. As illustrated in Figure S8a (Supporting Information), **fG** was heated in ethylenediamine according to the reported procedure, which affords **fG-Sub** after workup.[27] However, for **fG-Sub**, the element N (Supporting Information, Figure S9) cannot be seen in the "OMD" pattern using SEM-EDS, while the F signal (Supporting Information, Figure S8b) resembles that in Figure 2d; this behavior is not compatible with **Config-b**.[27,28]

This leaves **Config-c** as the most plausible scenario. Further strong support for **Config-c** stems from wettability experiments on the top side (Figure 6); the pristine graphene shows a static water contact angle of 96.7°. After fluorination of the entire area on the bottom side, the contact angle

 © 2020 The Authors. Published by Wiley-VCH Verlag GmbH & Co. KGaA, Weinheim

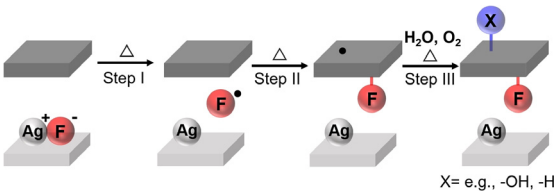

Scheme 3. Illustration of the proposed reaction mechanism of the bottom-side fluorination of graphene with AgF upon heating.

measured on the top side of this graphene becomes 88.4°, demonstrating enhanced hydrophilicity compared to that of pristine graphene. The results support **Config-c** with moieties such as oxygen-containing groups or hydrogen atoms on the top side. Furthermore, the presence of hydroxy groups is supported by the reaction of **fG** with $SOCl_2$ (Supporting Information, Figure S10). In contrast, for **Config-b** with fluorine terminals on the top side, a more hydrophobic surface is obtained compared to pristine graphene.[29]

A fluorination reaction mechanism is suggested (Scheme 3) based on the aforementioned results. Firstly, thermal decomposition of AgF generates Ag metal and F radicals (Step I).[30,31] The highly active F radicals attack the graphene, fluorinating the bottom side and generating dangling bonds (radical centers) on the opposite side at the

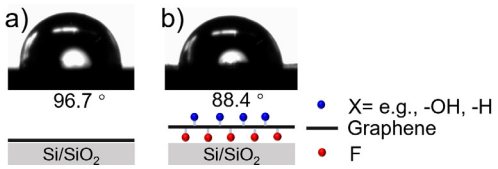

Figure 6. Wettability of the top side of a) pristine graphene and b) graphene with fluorination of the entire area on the bottom side.

same tune (Step II). Carbon radicals have been reported to react with H_2O or O_2 to afford hydroxylation or hydrogenation.[32,33] In our case, these reactive carbon radicals on graphene can undergo attacks by, for example, H_2O or O_2 (ambient or imported during the graphene transfer process) antaratopically to the fluorine atoms already bound (Step III). We have recently shown that an antaratopic 1,2-addition mode provides, by far, the thermodynamically most stable scenario.[17] Hence, the very high degree of functionalization at the patterned area can be attributed to the ditopic (antaratopic) addition mode; that is, fluorine atoms occupy the bottom side and moieties such as oxygen-containing groups or hydrogen atoms bind on the top side, giving rise to **Config-c** (Figure 4c).

In summary, a new method titled "2D substrate patterning" was developed for patterned functionalization of graphene by trapping the mild fluorination agent AgF in structured channels on the substrate. This facile method is quite efficient and can be easily extended to other systems by using other reactants. For the first time, patterned functionalization on the bottom side of graphene was realized by resolving the spatial hindrance from the substrate using our new method. The chemical patterning was performed with a high degree of functionalization and precise control, as visualized with Raman spectroscopy and SEM-EDS mapping. Moreover, the chemical nature of this patterned derivatization was demonstrated to be ditopic with fluorine atoms binding on the bottom side and moieties such as oxygen-containing groups or hydrogen atoms quenching on the top side. Accordingly, the reaction mechanism of the functionalization process is clearly disclosed. Our work provides a new facile method for patterned graphene functionalization and graphene fluorination, thereby freeing up the top side of graphene for many possibilities and enabling applications in graphene-based devices.

Acknowledgements

This work was supported by the Alexander von Humboldt (AvH) Foundation (L.B.) and funded by the Deutsche Forschungsgemeinschaft (DFG, German Research Foundation; Projektnummer 182849149, SFB 953). B.Z. is grateful for financial support from the China Scholarship Council (CSC).

Conflict of interest

The authors declare no conflict of interest.

Keywords: ditopic functionalization · fluorination · graphene · substrate patterning

How to cite: *Angew. Chem. Int. Ed.* **2020**, *59*, 6700–6705
Angew. Chem. **2020**, *132*, 6766–6771

[1] G. Bottari, M. Á. Herranz, L. Wibmer, M. Volland, L. Rodríguez-Pérez, D. M. Guldi, A. Hirsch, N. Martín, F. D'Souza, T. Torres, *Chem. Soc. Rev.* **2017**, *46*, 4464–4500.
[2] Y. Zhu, S. Murali, W. Cai, X. Li, J. W. Suk, J. R. Potts, R. S. Ruoff, *Adv. Mater.* **2010**, *22*, 3906–3924.
[3] C. K. Chua, M. Pumera, *Chem. Soc. Rev.* **2013**, *42*, 3222.
[4] V. Georgakilas, M. Otyepka, A. B. Bourlinos, V. Chandra, N. Kim, K. C. Kemp, P. Hobza, R. Zboril, K. S. Kim, *Chem. Rev.* **2012**, *112*, 6156–6214.
[5] Y. Zhou, K. P. Loh, *Adv. Mater.* **2010**, *22*, 3615–3620.
[6] L. Zhang, S. Diao, Y. Nie, K. Yan, N. Liu, B. Dai, Q. Xie, A. Reina, J. Kong, Z. Liu, *J. Am. Chem. Soc.* **2011**, *133*, 2706–2713.
[7] A. George, S. Mathew, R. van Gastel, M. Nijland, K. Gopinadhan, P. Brinks, T. Venkatesan, J. E. ten Elshof, *Small* **2013**, *9*, 711–715.
[8] W. Niu, J. Liu, Y. Mai, K. Müllen, X. Feng, *Trends Chem.* **2019**, *1*, 549–558.
[9] Z. Sun, C. L. Pint, D. C. Marcano, C. Zhang, J. Yao, G. Ruan, Z. Yan, Y. Zhu, R. H. Hauge, J. M. Tour, *Nat. Commun.* **2011**, *2*, 559.
[10] J. Li, M. Li, L.-L. Zhou, S.-Y. Lang, H.-Y. Lu, D. Wang, C.-F. Chen, L.-J. Wan, *J. Am. Chem. Soc.* **2016**, *138*, 7448–7451.
[11] S. Bian, A. M. Scott, Y. Cao, Y. Liang, S. Osuna, K. N. Houk, A. B. Braunschweig, *J. Am. Chem. Soc.* **2013**, *135*, 9240–9243.
[12] W. H. Lee, J. W. Suk, H. Chou, J. Lee, Y. Hao, Y. Wu, R. Piner, D. Akinwande, K. S. Kim, R. S. Ruoff, *Nano Lett.* **2012**, *12*, 2374–2378.

 © 2020 The Authors. Published by Wiley-VCH Verlag GmbH & Co. KGaA, Weinheim

[13] D. Ye, S.-Q. Wu, Y. Yu, L. Liu, X.-P. Lu, Y. Wu, *Appl. Phys. Lett.* **2014**, *104*, 103105.
[14] W.-K. Lee, K. E. Whitener, J. T. Robinson, P. E. Sheehan, *Adv. Mater.* **2015**, *27*, 1774 – 1778.
[15] L. G. Cançado, A. Jorio, E. H. M. Ferreira, F. Stavale, C. A. Achete, R. B. Capaz, M. V. O. Moutinho, A. Lombardo, T. S. Kulmala, A. C. Ferrari, *Nano Lett.* **2011**, *11*, 3190 – 3196.
[16] R. A. Schäfer, K. Weber, M. Koleśnik-Gray, F. Hauke, V. Krstić, B. Meyer, A. Hirsch, *Angew. Chem. Int. Ed.* **2016**, *55*, 14858 – 14862; *Angew. Chem.* **2016**, *128*, 15080 – 15084.
[17] K. Amsharov, D. I. Sharapa, O. A. Vasilyev, M. Oliver, F. Hauke, A. Goerling, H. Soni, A. Hirsch, *Carbon* **2019**, https://doi.org/10.1016/j.carbon.2019.11.008.
[18] K. C. Knirsch, R. A. Schäfer, F. Hauke, A. Hirsch, *Angew. Chem. Int. Ed.* **2016**, *55*, 5861 – 5864; *Angew. Chem.* **2016**, *128*, 5956 – 5960.
[19] A. Hirsch, F. Hauke, *Angew. Chem. Int. Ed.* **2018**, *57*, 4338 – 4354; *Angew. Chem.* **2018**, *130*, 4421 – 4437.
[20] L. Zhang, J. Yu, M. Yang, Q. Xie, H. Peng, Z. Liu, *Nat. Commun.* **2013**, *4*, 1443.
[21] I. Jeon, M. D. Peeks, S. Savagatrup, L. Zeininger, S. Chang, G. Thomas, W. Wang, T. M. Swager, *Adv. Mater.* **2019**, *31*, 1900438.
[22] R. R. Nair, W. Ren, R. Jalil, I. Riaz, V. G. Kravets, L. Britnell, P. Blake, F. Schedin, A. S. Mayorov, S. Yuan, M. I. Katsnelson, H. M. Cheng, W. Strupinski, L. G. Bulusheva, A. V. Okotrub, I. V. Grigorieva, A. N. Grigorenko, K. S. Novoselov, A. K. Geim, *Small* **2010**, *6*, 2877 – 2884.
[23] K. Tahara, T. Iwasaki, A. Matsutani, M. Hatano, *Appl. Phys. Lett.* **2012**, *101*, 163105.
[24] S. B. Bon, L. Valentini, R. Verdejo, J. L. Garcia Fierro, L. Peponi, M. A. Lopez-Manchado, J. M. Kenny, *Chem. Mater.* **2009**, *21*, 3433 – 3438.
[25] V. Mazánek, O. Jankovský, J. Luxa, D. Sedmidubský, Z. Janoušek, F. Šembera, M. Mikulics, Z. Sofer, *Nanoscale* **2015**, *7*, 13646 – 13655.
[26] P. C. Lee, D. Meisel, *J. Phys. Chem.* **1982**, *86*, 3391 – 3395.
[27] R. Stine, J. W. Ciszek, D. E. Barlow, W.-K. Lee, J. T. Robinson, P. E. Sheehan, *Langmuir* **2012**, *28*, 7957 – 7961.
[28] K. E. Whitener, R. Stine, J. T. Robinson, P. E. Sheehan, *J. Phys. Chem. C* **2015**, *119*, 10507 – 10512.
[29] G. Hong, Y. Han, T. M. Schutzius, Y. Wang, Y. Pan, M. Hu, J. Jie, C. S. Sharma, U. Müller, D. Poulikakos, *Nano Lett.* **2016**, *16*, 4447 – 4453.
[30] T. Flóra, I. Gaál, *Thermochim. Acta* **1973**, *7*, 173 – 181.
[31] A. A. Goryunkov, V. Y. Markov, O. V. Boltalina, A. K. Abdul-Sada, R. Taylor, *J. Fluorine Chem.* **2001**, *112*, 191 – 196.
[32] P. Ausloos, J. Paulson, *J. Phys. Chem.* **1958**, *62*, 501 – 502.
[33] A. Mardyukov, E. Sanchez-Garcia, R. Crespo-Otero, W. Sander, *Angew. Chem. Int. Ed.* **2009**, *48*, 4804 – 4807; *Angew. Chem.* **2009**, *121*, 4898 – 4901.

Manuscript received: February 18, 2020
Accepted manuscript online: February 27, 2020
Version of record online: March 24, 2020

 © 2020 The Authors. Published by Wiley-VCH Verlag GmbH & Co. KGaA, Weinheim